Photochemical & Photobiological Sciences (2022) 21:645–658
https://doi.org/10.1007/s43630-021-00117-8

ORIGINAL PAPERS

Tryptanthrin derivatives as efficient singlet oxygen sensitizers

Daniela Pinheiro[1] · **Marta Pineiro**[1] · **J. Sérgio Seixas de Melo**[1]

Received: 24 June 2021 / Accepted: 14 October 2021 / Published online: 4 November 2021

Abstract

Halogenated tryptanthrin and aminotryptanthrin were synthesized from indigo or isatin precursors. Dibromo- and tetrabromo-tryptanthrin were obtained from indigo dyes following green chemistry procedures, through microwave-assisted synthesis in mild oxidation conditions. Spectral and photophysical properties of the compounds, including quantitative determination of all the different deactivation pathways of S_1 and T_1, were obtained in different solvents and temperatures. The triplet state (T_1) has a dominant role on the photophysical properties of these compounds, which is further enhanced by the halogens at the fused-phenyl rings. Substitution with an amino group, 2-aminotryptanthrin (TRYP-NH_2), leads a dominance of the radiative decay channel. Moreover, with the sole exception of TRYP-NH_2, $S_1 \sim \sim > T_1$ intersystem crossing constitutes the dominant route, with internal conversion playing a minor role in the deactivation of S_1 in all the studied derivatives. In agreement with tryptanthrin, emission of the triplet state of tryptanthrin derivatives (with exception of TRYP-NH_2), was observed together with an enhancement of the singlet oxygen sensitization quantum yield: from 70% in tryptanthrin to 92% in the iodine derivative. This strongly contrasts with indigo and its derivatives, where singlet oxygen sensitization is found inefficient.

Graphic abstract

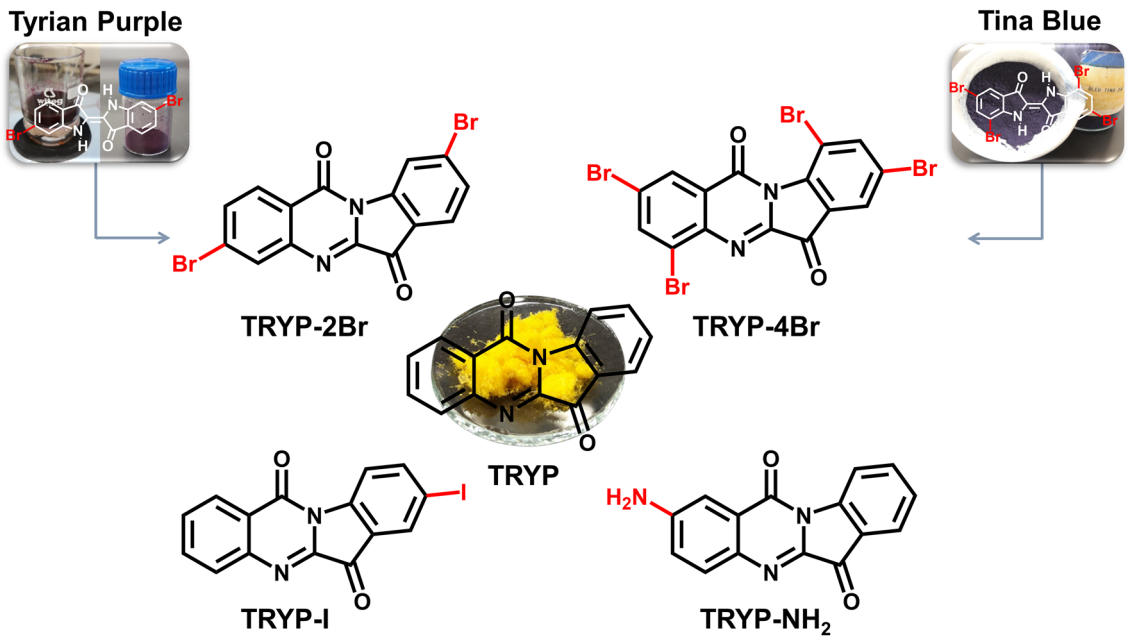

Keywords Tryptanthrin · Tryptanthrin derivatives · Fluorescence · Singlet oxygen sensitization

✉ J. Sérgio Seixas de Melo
sseixas@ci.uc.pt

[1] Department of Chemistry, CQC, University of Coimbra, Rua Larga, 3004-535 Coimbra, Portugal

1 Introduction

Tryptanthrin (indolo[2,1-*b*]quinazoline-6,12-dione), abbreviated as TRYP, is a natural compound found in diversified natural sources [1–6] and with several applications. Besides the extraction from natural sources, tryptanthrin can also be synthetically obtained from indigo or isatin increasing the structural diversity of tryptanthrin derivatives [7–11]. To increase the bioactivity of TRYP, several structural modifications have been accomplished. In the past recent years different TRYP derivatives [12–18] as well as its nanoformulations [19] have been synthetized and evaluated for potential biological and pharmacological activity, *e.g.* antipathogenic, antifungal, antiparasitic, antitubercular, antimalarial, anticancer, antioxidant, and anti-inflammatory [13, 20–29] and, very interesting, as stable active materials for all-organic redox flow batteries [30]. Most of these studies revealed that modification of TRYP core is important to develop novel and widespread potential applications in various fields. Moreover, encapsulation of TRYP in various nanoparticles [31] improves its delivery and its sustained release. These unique properties have led to obtain tryptanthrin derivatives that absorb and emit even at longer wavelength (wavelengths that are desirable for applications in biological systems) as well as fluorescent chemosensors for metal ions [32–38].

Recently the role of *N,N*'-dimethylformamide (DMF) to act as solvent and oxygen source in the formation of TRYP from indigo was investigated [39], this showed a new approach for the synthesis of TRYP from indigo via oxidation to isatin and subsequent oxidative cyclization by using the *trio* – sodium hydride (NaH), an iodine source and DMF under microwave irradiation [7, 39]. The developed methodology allows the synthesis of new tryptanthrin derivatives from well-known and available indigo dyes. Tyrian purple (6,6'-dibromoindigo or Royal purple) and Tina blue (5,5',7,7'-tetrabromoindigo, also known as Ciba Blue or Vat Blue 5), were successfully transformed into the corresponding di- and tetra-bromotryptanthrin derivatives. Monosubstituted tryptanthrin derivatives were obtained from the corresponding isatin or isatoic anhydride precursor through condensation, Chart 1. The comprehensive study of the electronic spectral and photophysical behaviour in solution of this set of tryptanthrin derivatives, including its singlet oxygen sensitization quantum yield clarify the interaction of this class of compounds with light, reveals its differences with indigo parents and open the way to their application as oxygen sensitizers.

Chart 1 Structures and acronyms of tryptanthrin (TRYP) and the studied tryptanthrin derivatives

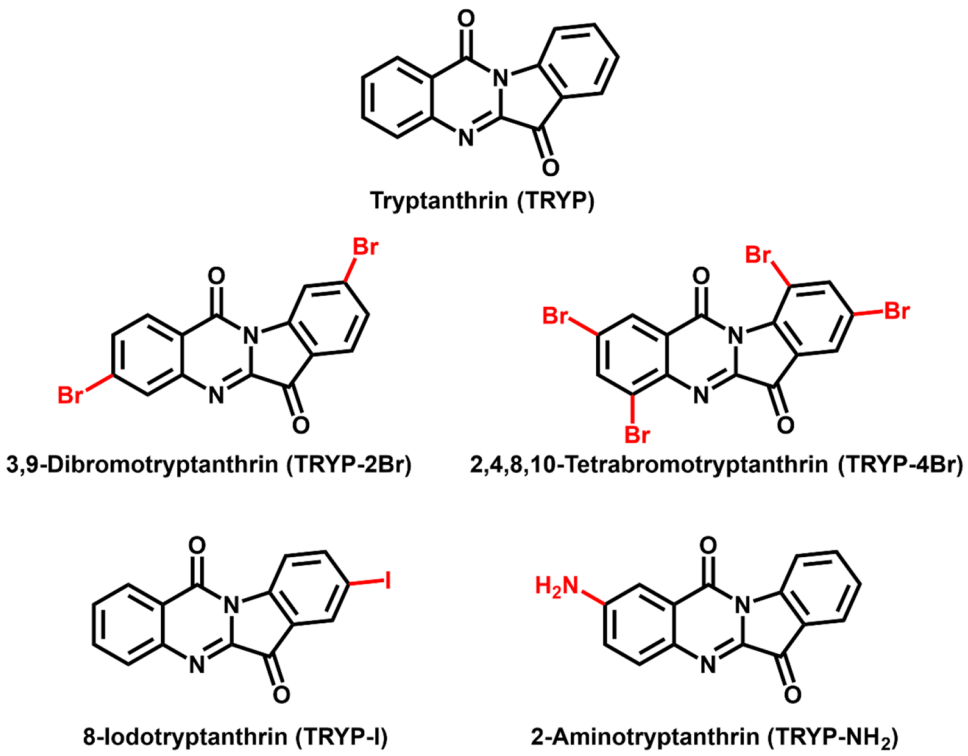

2 Experimental section

2.1 Materials

All the reagents for the synthesis, 1,2-diiodoethane, 4-bromo-2-nitrobenzaldehyde, 5-aminoisatoic anhydride, sodium hydride (60% dispersion in mineral oil, stored in a dry box) were obtained from Sigma-Aldrich, 5-iodoisatin and Ciba Blue 2B (Tina Blue) were purchased from TCI Chemicals and isatoic anhydride and isatin from Merck. All

reagents used for the synthesis of the compounds were used without further purification. For the synthetic procedures, the solvents were of commercial pro analysis (P.A.) grade. For the spectral and photophysical determinations, the solvents used were of spectroscopic or equivalent grade.

2.2 Equipment and methods

Microwave (MW)-assisted reactions were performed in a CEM Discover S-Class single-mode microwave reactor, featuring continuous temperature, pressure and microwave power monitoring.

Analytical thin-layer chromatography (TLC) was performed on Macherey–Nagel ALUGRAM Xtra silica gel plates with UV_{254} indicator. Visualization was accomplished by using an ultraviolet lamp. Silica gel column was carried out with silica gel (230–400 mesh).

Nuclear magnetic resonance (NMR) spectra were recorded at room temperature in deuterated chloroform ($CDCl_3$) solutions on a Bruker Avance III spectrometer and a Bruker DRX-400 spectrometer, operating at 400.13 MHz for ^1H and 100.61 MHz for ^{13}C, and are given in Figures SI1-8 in SI. Chemical shifts (δ) for ^1H and ^{13}C are expressed in ppm, relatively to an internal standard of TMS (tetramethylsilane). Coupling constants (*J*) are indicated in Hz.

Gas chromatography-mass spectroscopy (GC–MS) analyses were performed on a Hewlett-Packard 5973 MSD spectrometer, using electron ionization (EI) (70 eV), coupled with a Hewlett-Packard Agilent 6890 chromatography system, equipped with a HP-5 MS column (30 m × 0.25 mm × 0.25 µm) and high-purity helium as carrier gas. The initial temperature of 70 °C was increased to 250 °C at a 15 °C min^{-1} rate, and held for 10 min. Then the temperature was increased to 290 °C at a 5 °C min^{-1} rate and held for 2 min, giving a total run time of 32 min. The flow of the carrier gas was maintained at 1.33 mL min^{-1}. The injector port was set at 250 °C.

High resolution mass spectrometry (HRMS) was performed either on a Bruker microTOF-Focus mass spectrometer equipped with an electrospray ionization time-of-flight (ESI-TOF) source or a Waters-Micromass GC-TOF mass spectrometer equipped with an electron ionization (EI) source. Experimental (red line) and calculated (green line) high resolution mass spectra are given in Figure SI9-12 in SI.

Absorption and fluorescence spectra were recorded on a Shimadzu UV-2450 and Horiba-Jobin-Ivon SPEX Fluorolog 3–22 spectrometers, respectively. Fluorescence spectra were corrected for the wavelength response of the system. For the steady state and time resolved emission experiments, the absorption at the excitation wavelength was kept below 0.1 values to avoid inner-filter, reabsorption or aggregation effects.

The singlet extinction coefficients (ε_{SS}) were obtained from the slope of the plot of the absorption with (at least) five solutions in the range concentration 5×10^{-5}–6×10^{-6} mol L^{-1} *versus* the concentration (correlation values ≥ 0.999) (see Figure SI13 in SI).

The fluorescence quantum yields (ϕ_F) at room temperature (293 K) were measured by the comparative method using the absolute ϕ_F values obtained for TRYP in each solvent [7] as standard using the equation bellow (Eq. 1):

$$\phi_F^{cp} = \frac{\int I^{cp}(\lambda)\, d\lambda}{\int I^{ref}(\lambda) d\lambda} \cdot \frac{n_{cp}^2}{n_{ref}^2} \cdot \phi_F^{ref} \quad (1)$$

where $\int I^{cp}(\lambda) d\lambda$ is the integrated area under the emission spectra of the compound (*cp*) in solution and $\int I^{ref}(\lambda) d\lambda$ of the reference (*ref*) in solution, n_{cp}^2 and n_{ref}^2 are the refractive index of the solvents in which the compound and reference were dissolved, respectively and ϕ_F^{ref} is the fluorescence quantum yield of the standard. The fluorescence quantum yields were obtained with optically matched solutions, at the excitation wavelength, of tryptanthrin derivatives and TRYP.

Phosphorescence measurements were recorded with a Horiba-Jobin-Ivon SPEX Fluorolog 3–22 spectrometer using a 150 W pulsed Xenon lamp. The phosphorescence spectra were corrected for the wavelength response of the system. Phosphorescence experiments were performed with a quartz NMR-like (EPR) tube. Due to the smaller optical pathway, *l*, an absorbance of ~ 0.4 (with a 1 cm optical length cuvette) was used in contrast to the ~ 0.1 used in fluorescence experiments. This tube was put inside a dewar (fixed to the equipment with an appropriate holder) filled up with liquid nitrogen.

The phosphorescence quantum yields were determined using biacetyl ($\phi_{Ph} = 0.23$) [40] in a mixed solvent containing diethyl ether, isopentane and ethanol in a 5:5:2 (v/v/v) ration as standard [41].

Singlet oxygen formation quantum yields (ϕ_Δ) were obtained by direct measurements of the phosphorescence emission spectrum of singlet oxygen, $^1O_2$, centered at 1275 nm with a Horiba-Jobin-Ivon SPEX Fluorolog 3–22 spectrometer equipped with a near-infrared (NIR) detector Hamamatsu R5509-42 photomultiplier cooled to 193 K in a liquid nitrogen chamber. To avoid the overlap of the fluorescence emission second harmonic signal with the sensitized singlet oxygen phosphorescence emission at 1275 nm a Newport long-pass dielectric filter with 1000 nm cut-on (reference 10LWF-1000-B) was used. The sensitized phosphorescence emission spectra of $^1O_2$ from optically matched solutions of the samples and that of the reference compound were obtained in identical experimental conditions (ΔOD = 0.20–0.30). The singlet oxygen formation quantum yield was then determined by comparing the integrated area under the emission spectra of the sample solutions

($\int I^{cp}(\lambda)d\lambda$) and that of the reference solution ($\int I^{ref}(\lambda)d\lambda$) and applying the equation (Eq. 2) [42],

$$\phi_{\Delta}^{cp} = \frac{\int I^{cp}(\lambda)d\lambda}{I^{ref}(\lambda)\lambda d\lambda}.\phi_{\Delta}^{ref} \quad (2)$$

with ϕ_{Δ}^{ref} the singlet oxygen formation quantum yield of the reference compound. 1H-phenalen-1-one in acetonitrile ($\phi_{\Delta} = 0.98$) as used as standard [43]. Singlet oxygen formation quantum yields were obtained with optically matched solutions, at the excitation wavelength, of tryptanthrin derivatives and 1*H*-phenalen-1-one.

Fluorescence decays were measured using a home-built picosecond time-correlated single photon counting (ps-TCSPC) apparatus described elsewhere [44]. The excitation source consists of a tunable picoseconds Spectra-Physics mode-lock Tsunami laser (Ti:Sapphire) model 3950 (80 MHz repetition rate, tuning range 700–1000 nm), pumped by a 532 nm continuous wave Spectra-Physics Millennia Pro-10 s laser.

The fluorescence decays and the instrumental response function (IRF) were collected using a time scale corresponding to 1024 channels in a 4.44 or 24.4 ps/channel scale (chosen according to the time scale of the fluorescence decay). The excitation wavelengths used in this work (λ_{exc} = 422 nm) were obtained with a Spectra-Physics harmonic generator, model GWU-23PS with time resolution ~ 2 ps after deconvolution of the signal (the pulse instrument response is typically of ~ 20 ps). When a PicoQuant Picosecond Laser Diode Head, picoLED, model LDH-P–C-450B with λ_{exc} = 451 nm was used as excitation source, the pulse instrumental response is larger and the time resolution is also lower (*ca.* 20 ps). The fluorescence decay curves were analysed by deconvolution using the IRF signal collected with a scattering solution (aqueous Ludox solution). Deconvolution of the decays was performed using the modulation function method, as implemented by George Striker in the SAND program and elsewhere described [45]. Nanosecond transient absorption (ns-TA) spectra were measured with an Applied Photophysics laser flash photolysis equipment pumped by the third harmonic (355 nm) of a Nd:YAG laser (Spectra Physics). The detection was obtained with an Hamamatsu R928 photomultiplier and a pulsed 150 W Xe lamp, which were used to analyze the transient absorption. The transient spectra were collected by monitoring the optical density change at intervals of 5–10 nm, averaging at least 10 decays at each wavelength.

2.3 Synthesis of halogenated tryptanthrin derivatives

2.3.1 Synthesis of Tyrian purple (6,6′-dibromoindigo)

Tyrian purple was synthesized via the Baeyer–Drewsen reaction following a similar procedure for the synthesis of indigo [46, 47]. Using 4-bromo-2-nitrobenzaldehyde as starting material Tyrian was obtained in moderate yields, see Scheme SI1. 4-Bromo-2-nitrobenzaldehyde (200 mg) was dissolved in acetone (10 mL) and 10 mL of water was added in small amounts keeping an inert atmosphere (N_2) and cooling the reaction in an ice bath. 2.0 M aqueous sodium hydroxide solution was added dropwise keeping the pH at 10, until the complete formation of a dark precipitate. The suspension was stirred overnight. The purple precipitate was filtered off, washed several times with acetone and water (3 × 20 mL) and dried over vacuum, yielding 105 mg (29% yield) of 6,6'-dibromoindigo (Tyrian purple). Due to the insolubility of Tyrian purple in various deuterated solvents the ^{1}H and ^{13}C NMR spectra were not collected. **EI-TOF–MS:** m/z $[M+1]^+$ = 419.8923 calculated for $C_{16}H_9Br_2N_2O_2$; found: 419.8932.

2.3.2 Synthesis of 3,9-dibromoindolo[2,1-b] quinazoline-6,12-dione, 3,9-dibromotryptanthrin (TRYP-2Br)

In a thick-glass microwave reactor, with a magnetic stirring bar, Tyrian purple (80 mg, 1 equiv) and sodium hydride (NaH) (2 equiv) were dissolved in 1 mL of dry *N,N'*-dimethylformamide (DMF). Then, 1,2-diiodoethane (2 equiv) and DMF were added to a total volume of 2 mL. The resulting mixture was heated under microwave irradiation at 50 °C for 15 min. The crude was extracted with dichloromethane and purified by column chromatography (SiO_2) using ethyl acetate/ hexane (1:3; v/v) as eluent to yield TRYP-2Br as a yellow solid (29 mg, 37% yield). **^{1}H NMR ($CDCl_3$, 400 MHz),** 8.85 (d, *J* = 1.5 Hz, 1H), 8.29 (d, *J* = 8.5 Hz, 1H), 8.19 d, *J* = 1.8 Hz, 1H), 7.81–7.76 (m, 2H), 7.61 (dd, *J* = 1.6 Hz, *J* = 8.1 Hz, 1H) ppm. **^{13}C NMR ($CDCl_3$, 101 MHz)**, δ 180.0, 156.4, 146.5, 145.5, 143.9, 132.7, 132.7, 132.4, 129.9, 129.2, 127.9, 125.3, 121.3, 120.4, 119.5 ppm. **GC–MS:** m/z $[M^+]$ = 405.9. **ESI-TOF–MS:** m/z $[M+1]^+$ = 404.8869 calculated for $C_{15}H_7Br_2N_2O_2$; found: 404.4886.

2.3.3 Synthesis of 2,4,8,10-tetrabromoindolo[2,1-b] quinazoline-6,12-dione, 2,4,8,10-tetrabromotryptanthrin (TRYP-4Br)

In a thick-glass microwave reactor charged with a magnetic stirring bar, 5,5',7,7'-tetrabromoindigo (Tina Blue) (200 mg, 1 equiv) and NaH (2 equiv) were dissolved in 1 mL of dry

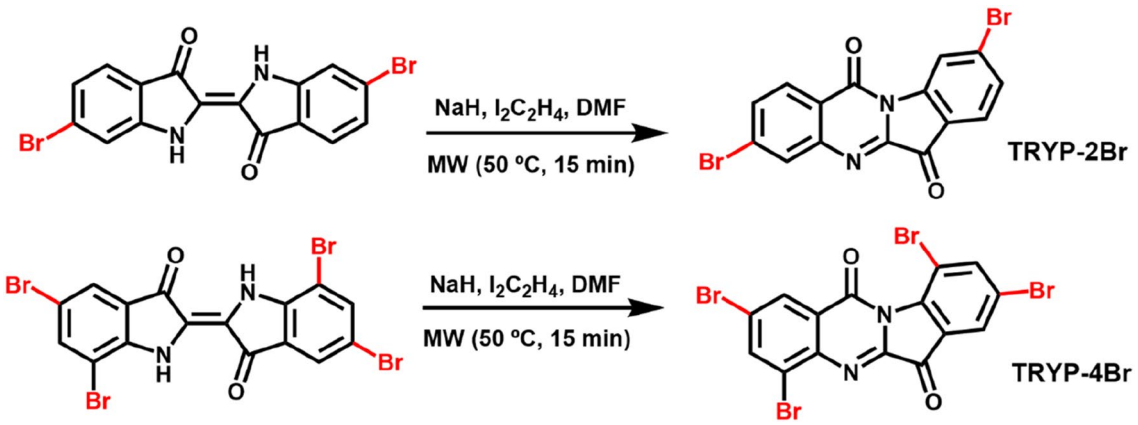

Scheme 1 Schematic pathways for the synthesis of 3,9-dibromotryptanthrin (TRYP-2Br) from Tyrian purple and 2,4,8,10-tetrabromotryptanthrin (TRYP-4Br) from Tina blue

DMF. 1,2-diiodoethane (2 equiv) and DMF were added to a total volume of 2 mL. The resulting mixture was heated under microwave irradiation at 50 °C for 15 min. After cooling down to room temperature, the reaction mixture was extracted with dichloromethane and water and the organic layer was dried over anhydrous sodium sulfate overnight. The mixture was then filtered and the solvent concentrated under reduce pressure. The crude was purified by column chromatography (SiO_2) using ethyl acetate/ hexane (1:3; v/v) as eluent to yield TRYP-4Br as a light green solid (36 mg, 18% yield). **^{1}H NMR ($CDCl_3$, 400 MHz),** 8.43 (d, J = 2.1 Hz, 1H), 8.22 (d, J = 2.2 Hz, 1H), 8.15 (d, J = 1.9 Hz, 1H), 8.03 (d, J = 1.9 Hz, 1H) ppm. **^{13}C NMR (CDCl3, 101 MHz)**, δ 179.4, 154.7, 145.7, 144.6, 144.5, 143.0, 141.4, 130.0, 127.5, 127.3, 126.7, 126.5, 124.8, 122.0, 112.04 ppm. **ESI-TOF–MS:** m/z $[M+1]^+$ = 560.7079 calculated for $C_{15}H_5Br_4N_2O_2$; found: 560.7074.

2.3.4 Synthesis of 8-iodoindolo[2,1-b] quinazoline-6,12-dione, 8-iodotryptanthrin (TRYP-I) and 2-aminoindolo[2,1-b]quinazoline-6,12-dione, 2-aminotryptanthrin (TRYP-NH_2)

Mono-substituted tryptanthrin derivatives were synthesized following a previously reported procedure [15]. Briefly, a solution of isatin (500 mg, 1 equiv) in 10 mL of DMF was added over a 15 min period to NaH solution (43 mg, 1 equiv) with stirring. To the resulting purple liquid, isatoic anhydride (323 mg, 1.1 equiv) in 10 mL of DMF was added keeping the reaction on ice over a 30 min period. The reaction mixture was stirred 48 h at room temperature and then quenched with 10 mL of methanol. The resulting mixture was diluted with 50 mL of chloroform and washed once with water. The aqueous layer was extracted three times with chloroform and the combined organic layers were concentrated under reduce pressure. Crystallization from acetone afforded the pure tryptanthrin derivatives.

TRYP-I: yellow solid (626 mg, 93% yield). **^{1}H NMR ($CDCl_3$, 400 MHz),** 8.45–8.46 (m, 2H), 8.21 (dd, J = 1.7 Hz, 1H), 8.08 (dd, J = 1.8 Hz, J = 8.5 Hz, 1H), 8.02 (d, J = 7.9 Hz, 1H), 7.86 (dt, J = 1.6 Hz, J = 7.2 Hz, 1H), 7.68 (dt, J = 1.2 Hz, J = 7.2 Hz, 1H) ppm. **^{13}C NMR (DMSO-d_6, 101 MHz)**, 180.8, 157.9, 149.2, 146.1, 145.6, 145.2, 135.8, 132.6, 130.3, 130.1, 127.2, 123.1, 122.8, 119.5, 117.7 ppm. **ESI-TOF–MS:** m/z $[M+1]^+$ = 374.9625 calculated for $C_{15}H_8IN_2O_2$; found: 374.9629.

TRYP-NH_2: dark brown solid (734 mg, 82% yield). **^{1}H NMR (400 MHz, $CDCl_3$)**, δ 8.86 (d, J = 8.9 Hz, 1H), 8.76 (d, J = 2.1 Hz, 1H), 8.69 (dd, J = 2.2 Hz, J = 8.9 Hz, 1H), 8.48 (d, J = 7.3 Hz, 1H), 8.07 (d, J = 8.0 Hz, 1H), 7.92 (dt, J = 1.2 Hz, J = 6.8 Hz, 1H), 7.74 (t, J = 7.4 Hz, 1H) ppm.**^{13}C NMR (CDCl3, 101 MHz)**, δ 181.1, 157.6, 146.4, 145.5, 145.2, 144.5, 135.3, 132.6, 130.0, 130.0, 127.0, 124.2, 123.1, 119.0, 91.4 ppm. **ESI-TOF–MS:** m/z $[M+1]^+$ = 264.0768 calculated for $C_{15}H_{10}N_3O_2$; found: 264.0770.

3 Results and discussion

3.1 Synthesis of tryptanthrin derivatives

The two bromo tryptanthrin derivatives, 3,9-dibromotryptanthrin (TRYP-2Br) and 2,4,8,10-tetrabromotryptanthrin (TRYP-4Br), were successful synthesized from Tyrian purple and Tina blue, respectively. The synthetic methodology previously developed by our research group [7, 39] for the synthesis of TRYP from indigo, allows the synthesis of tryptanthrins with two or four bromine atoms from the respective indigo dyes. Using the oxidant system formed by the *trio*–NaH, 1,2-diodoethane and DMF and microwave irradiation [39], the limitative characteristic of low

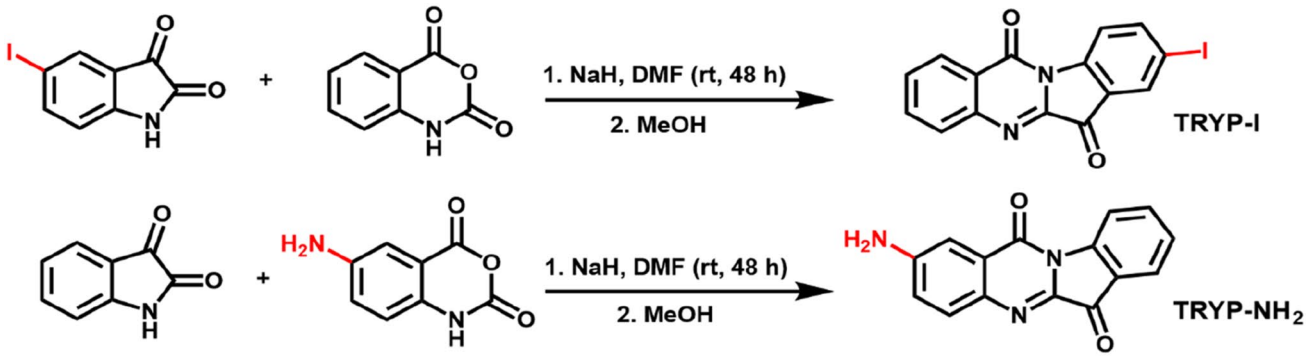

Scheme 2 Synthesis of 8-iodotryptanthrin (TRYP-I) and 2-aminotryptanthrin (TRYP-NH_2)

solubility of these indigo dyes in organic solvents was overcome and tryptanthrin analogues were obtained in moderate oxidative conditions and short reaction times, see Scheme 1. Even considering the relatively moderated reaction yields obtained using this methodology, the significant reduction on the amount of solvent needed to perform the reaction has a positive impact in the E-Factor (environmental factor [48]) decreasing from 187 –calculated for the synthesis of 3,9-dibromotryptanthrin from 5-bromoisatin and 5-bromoisatoic anhydride in 80% yield following the experimental procedure herein described for the synthesis of mono-substituted tryptanthrin derivatives – to 72, implying that a reduction of the mass of waste produce to less than a half has occurred (see Table SI1).

The two mono-substituted tryptanthrin derivatives, 8-iodotryptanthrin (TRYP-I) and 2-aminotryptanthrin (TRYP-NH_2), were obtained from the condensation of anthranilic acid derivatives, in particular isatoic anhydrides, with isatin in the presence of a base. The use of NaH instead of triethylamine [25] allows to obtain the desired product after 48 h at room temperature, in excellent yields after simple recrystallization (Scheme 2).

3.2 Excited state characterization

3.2.1 Absorption and steady state fluorescence spectral data

The absorption and fluorescence, emission and excitation, spectra of the tryptanthrin derivatives obtained at room temperature (T = 293 K) in acetonitrile (MeCN) are depicted in Fig. 1. Full spectra, including in other solvents (ethanol (EtOH) and methanol (MeOH)), are given in Figure SI14. Similarly to TRYP, the absorption spectra of the different tryptanthrin derivatives, with exception of TRYP-NH_2, remains relatively unaffected with the polarity and/or hydrogen bonding ability of the solvent [7]. Noteworthy is the different spectral behaviour of TRYP-NH_2, *i.e.*, absence of the absorption band at shorter wavelengths (~ 350 nm), see Fig. 1 and Figure SI14. It is also worth noting the broad emission spectra of the bromine and iodine tryptanthrin spectra, contrasting with the more narrowed nature of the TRYP-NH_2 spectrum.

Table 1 summarizes the spectral data for the studied tryptanthrin derivatives. Di-substitution with bromine atoms (TRYP-2Br) leads to a small blue shift in the fluorescence emission when compared with TRYP. Further increment on the degree of substitution with two more bromine atoms (TRYP-4Br), with an iodine atom (TRYP-I), or an amino group (TRYP-NH_2) leads to red-shifts of the emission (Table 1, Fig. 1).

The fluorescence emission spectra of TRYP and derivatives are found solvent dependent, with particular emphasis in TRYP-NH_2 where the large positive solvatochromism, of the fluorescence spectra, has been associated to an effective intramolecular charge transfer (ICT) character involving the carbonyl group of the five-membered ring and the amino group [49]. Additionally, for the four studied compounds molar absorption coefficients were found with the same order of magnitude, and typical of π-π* transitions, with $\varepsilon_{SS} \approx 10^3\ M^{-1}\ cm^{-1}$. These values are in agreement with those previously reported for tryptanthrin [7] and other tryptanthrin derivatives [36, 50, 51].

3.2.2 Photophysics: quantum yields

Data in Table 2 shows that substitution in the TRYP core influences the excited state deactivation pathways. Introduction of the amino group, TRYP-NH_2, leads to a high fluorescence quantum yield (ϕ_F) value and a relatively low (in comparison with the other three compounds studied) singlet oxygen sensitization yield (ϕ_Δ~0.1) and absence of phosphorescence emission.

Photophysical data in Table 2 show that the donor amino group, TRYP-NH_2, strongly facilitates the radiative deactivation route with solvent dependent fluorescence quantum

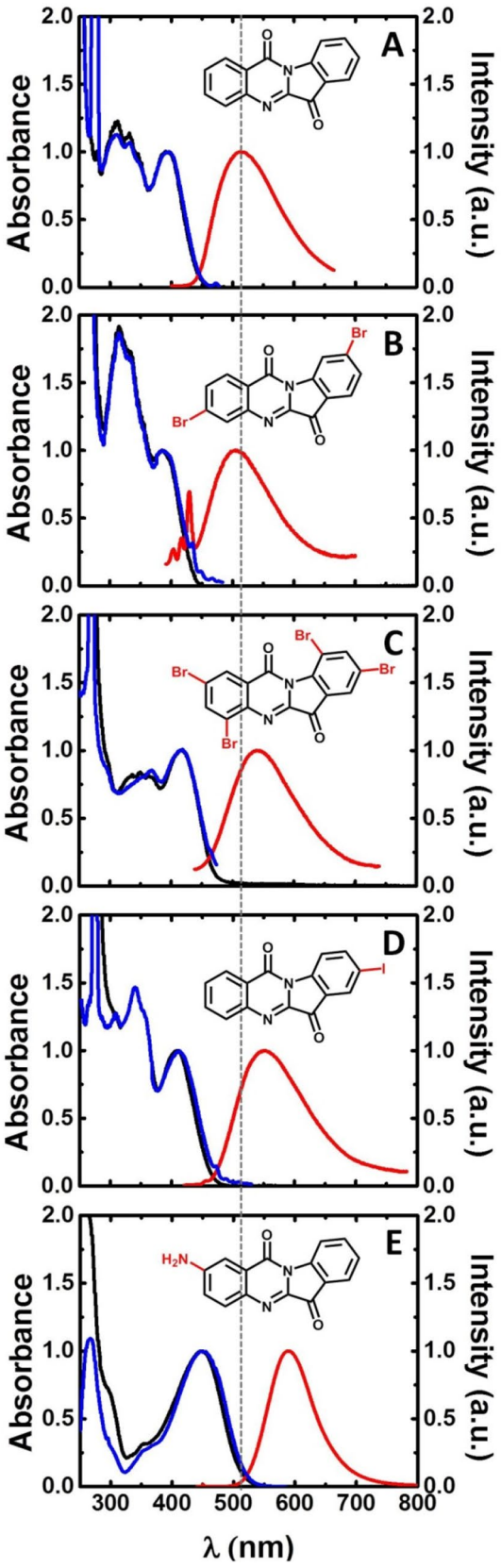

Fig. 1 Normalized absorption (black line), excitation (blue line) and fluorescence emission (red line) spectra for TRYP (**A**), TRYP-2Br (**B**), TRYP-4Br (**C**), TRYP-I (**D**) and TRYP-NH_2 (**E**) in MeCN solution at $T = 293$ K. The emission spectra were obtained with $\lambda_{exc} = 330–450$ nm and the excitation spectra with $\lambda_{em} = 500–590$ nm. The dashed vertical line is just meant to be a guideline to the eye in particular to the red-shift of the emission band

yields (ranging from 0.2 to 0.8). Introduction of the heavy atoms, iodine and bromine, strongly increases sensitization of singlet oxygen, via efficient spin–orbit coupling, with quantum yields, ϕ_Δ~90% (Table 2 and Figure SI15) in the order TRYP-I > TRYP-2Br ~ TRYP-4Br > TRYP [7]; this is followed by a decrease in the fluorescence quantum yields with values, for all the compounds, lower in polar protic solvents than in polar aprotic solvents, particularly evident for TRYP and TRYP-NH_2. Moreover, exception made to TRYP-NH_2, the triplet state formation quantum yields, ϕ_T –here assumed to be identical to the singlet oxygen yield, *i.e.*, $\phi_T \sim \phi_\Delta$– constitutes the dominant deactivation for all the tryptanthrin derivatives, with the internal conversion (IC) playing a minor role in the deactivation of the S_1 state in all the studied derivatives.

Characterization of the triplet state was further complemented with the determination of phosphorescence quantum yields and lifetimes. Figure 2 shows the phosphorescence emission spectra for TRYP-2Br, TRYP-4Br and TRYP-I collected in vitreous ethanol at $T = 77$ K. In agreement to what was observed for TRYP [7], the studied derivatives display a broad phosphorescence emission band, with two vibronic bands, that partially overlaps the fluorescence emission band (also collected at low temperature, 77 K), as illustrated in Figure SI16.

From Fig. 2, Table 2 it is seen that the phosphorescence quantum yields are generally low with values ranging from $\phi_{Ph} = 0.0027$ (TRYP) and $\phi_{Ph} = 0.038$ (TRYP-I). The low phosphorescence quantum yields and high quantum yields for singlet oxygen formation are associated with, the phosphorescence quantum yields obtained at 77 K (that strongly increases the radiative deactivation from T_1 at the expenses of the radiationless deactivation) whereas the singlet oxygen sensitization (and triplet state) quantum yields are obtained at room temperature.

Phosphorescence lifetimes were found in the ms time scale ($\tau_{Ph} < 0.01$ s), phosphorescence decays in Figure SI17, indicating the nature of the triplet state to be of n,π* origin [52]. The very efficient $S_1 \sim\sim > T_1$ process indicates, together with the small singlet–triplet energy gap ($\Delta E_{S\text{-}T} = 0.23$ eV–0.45 eV), see Table SI2, that according to El-Sayed rules [53], the interacting singlet (S_1) and triplet (T_n) are of different origin and, as with TRYP [7], S_1 is of π, π* origin.

Transient singlet–triplet difference absorption spectra of tryptanthrin and derivatives obtained by laser flash

Table 1 Spectral data including absorption (λ_{Abs}), fluorescence (λ_{Fluo}) and phosphorescence (λ_{Ph}) wavelength maxima, Stokes shifts (Δ_{SS}) and molar absorption coefficient (ε_{SS}) for TRYP and derivatives in solvents of different dielectric constant (ε), at $T = 293$ K and $T = 77$ K

Compound	Solvent	ε^b	λ_{Abs} (nm) (293 K)	λ_{Fluo} (nm) (293 K)	λ_{Ph} (nm) (77 K)	Δ_{SS} (cm^{-1}) (293 K)	ε_{SS} (M^{-1} cm^{-1}) (293 K)
TRYP[a]	**MeCN**	35.9	394	513	N.D.[c]	5888	3545
	EtOH	24.6	389	539	567, 615	7154	4169
	MeOH	32.7	389	552	N.D.[c]	7591	3736
TRYP-2Br	**MeCN**	35.9	386	506	N.D.[c]	6144	5197
	EtOH	24.6	383	534	561, 602	7383	4752
	MeOH	32.7	384	543	N.D.[c]	7625	4374
TRYP-4Br	**MeCN**	35.9	416	540	N.D.[c]	5520	8736
	EtOH	24.6	410	556	575, 629	6405	5660
	MeOH	32.7	410	567	N.D.[c]	6754	6973
TRYP-I	**MeCN**	35.9	410	551	N.D.[c]	6241	6812
	EtOH	24.6	407	573	575, 613	7118	3424
	MeOH	32.7	405	591	N.D.[c]	7771	4786
TRYP-NH_2	**MeCN**	35.9	450	590	–	5273	6935
	EtOH	24.6	475	631	–	5205	6737
	MeOH	32.7	463	639	–	5949	5732

[a]For TRYP data is from ref [7]

[b]Values are from ref [41]

[c]*N.D.* = Not determined

Table 2 Photophysical data including fluorescence (ϕ_F), phosphorescence (ϕ_{Ph}), intersystem crossing triplet through $^1O_2$ sensitization ($\phi_\Delta \approx \phi_T$) and internal conversion (ϕ_{IC}) quantum yields, fluorescence (τ_F) and phosphorescence lifetimes (τ_{Ph}) and rate constants (fluorescence (k_F), nonradiative (k_{NR}), internal conversion (k_{IC}) and intersystem crossing (k_{ISC})) for tryptanthrin derivatives in solvents of different dielectric constant (ε), at $T = 293$ K and $T = 77$ K. Data for TRYP is also presented for comparison

Compound	Solvent	ε^b	ϕ_F (293 K)	τ_F (ps)[c] (293 K)	ϕ_{Ph} (77 K)	τ_{Ph} (ms) (77 K)	$\phi_\Delta \approx \phi_T$[d] (293 K)	ϕ_{IC} (293 K)	k_F (ns^{-1})[e] (293 K)	k_{NR} (ns^{-1})[e] (293 K)	k_{IC} (ns^{-1})[e] (293 K)	k_{ISC} (ns^{-1})[e] (293 K)
TRYP[a]	**MeCN**	35.9	0.0084	499			0.77	0.22	0.017	1.987	0.440	1.547
	EtOH	24.6	0.0028	255	0.0027	10.34			0.011	3.911		
	MeOH	32.7	0.0019	146					0.013	6.836		
TRYP-2BR	**MeCN**	35.9	0.0027	109			0.91	0.090	0.025	9.150	0.828	8.322
	EtOH	24.6	0.0017	193	0.0215	4.52			0.009	5.173		
	MeOH	32.7	0.0018	174					0.010	5.737		
TRYP-4BR	**MeCN**	35.9	0.0015	119			0.84	0.16	0.013	8.391	1.241	7.150
	EtOH	24.6	0.0013	89	0.0063	4.34			0.015	11.221		
	MeOH	32.7	0.0011	68					0.016	14.690		
TRYP-I	**MeCN**	35.9	0.0011	82			0.92	0.080	0.013	12.182	0.901	11.280
	EtOH	24.6	0.0009	40	0.0384	1.23			0.023	24.978		
	MeOH	32.7	0.0008	41					0.020	24.371		
TRYP-NH_2	**MeCN**	35.9	0.81	2987			0.10	0.085	0.271	0.064	0.029	0.035
	EtOH	24.6	0.30	1144	–	–			0.258	0.616		
	MeOH	32.7	0.19	832					0.232	0.970		

[a]For TRYP data from ref [7]

[b]Values taken from ref [41]

[c]The decay time considered here is the longer component in the fluorescence decays

[d]Assuming efficient singlet oxygen photosensitization, $S_\Delta = \phi_\Delta/\phi_T \approx 1$, from the investigated sample

[e]$k_F = \frac{\phi_F}{\tau_F}; k_{NR} = \frac{1-\phi_F}{\tau_F}; k_{IC} = \frac{1-\phi_F-\phi_T}{\tau_F}; k_{ISC} = \frac{\phi_T}{\tau_F}; \phi_{IC} = 1 - \phi_F - \phi_T$

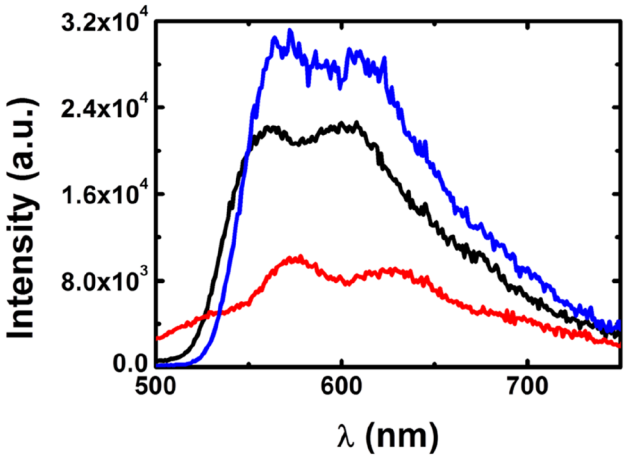

Fig. 2 Phosphorescence emission spectra of TRYP-2Br (black line), TRYP-4Br (red line) and TRYP-I (blue line) in vitreous EtOH at $T = 77$ K

photolysis with excitation at 355 nm in degassed MeCN solution are depicted in Fig. 3.

The transient lifetimes are found quenched by oxygen and thus the observed spectroscopic features are assigned to triplet excited state absorption. In the absence of oxygen all triplet lifetimes are found in the μs time range. The triplet lifetime for TRYP-I (Fig. 3D) is similar to the value of TRYP ($\tau_T \approx 2\mu s$) (Fig. 3A), while, the compounds TRYP-2Br (Fig. 3B) and TRYP-4Br (Fig. 3C) presented higher transient lifetimes ($\tau_T \approx 7\mu s$). Similar triplet lifetimes were found all over the transient difference absorption bands.

3.2.3 Photophysics: time-resolved fluorescence

Further insights of the decay mechanisms were obtained from time-resolved fluorescence experiments in oxygen and oxygen free solutions for the different tryptanthrin derivatives (Table 3 and Table SI3 in SI). With the exception of TRYP-I, similar results were found for the fluorescence lifetimes in oxygen and free oxygen solutions. For TRYP-I, it was found that for UV light irradiated N_2 degassed solutions the colour changes from yellow to orange (Figure SI18). The decomposition of organic compounds containing iodine in solution by UV light has been the subject of some investigations and it has been shown that iodine is released after UV light irradiation [54, 55].

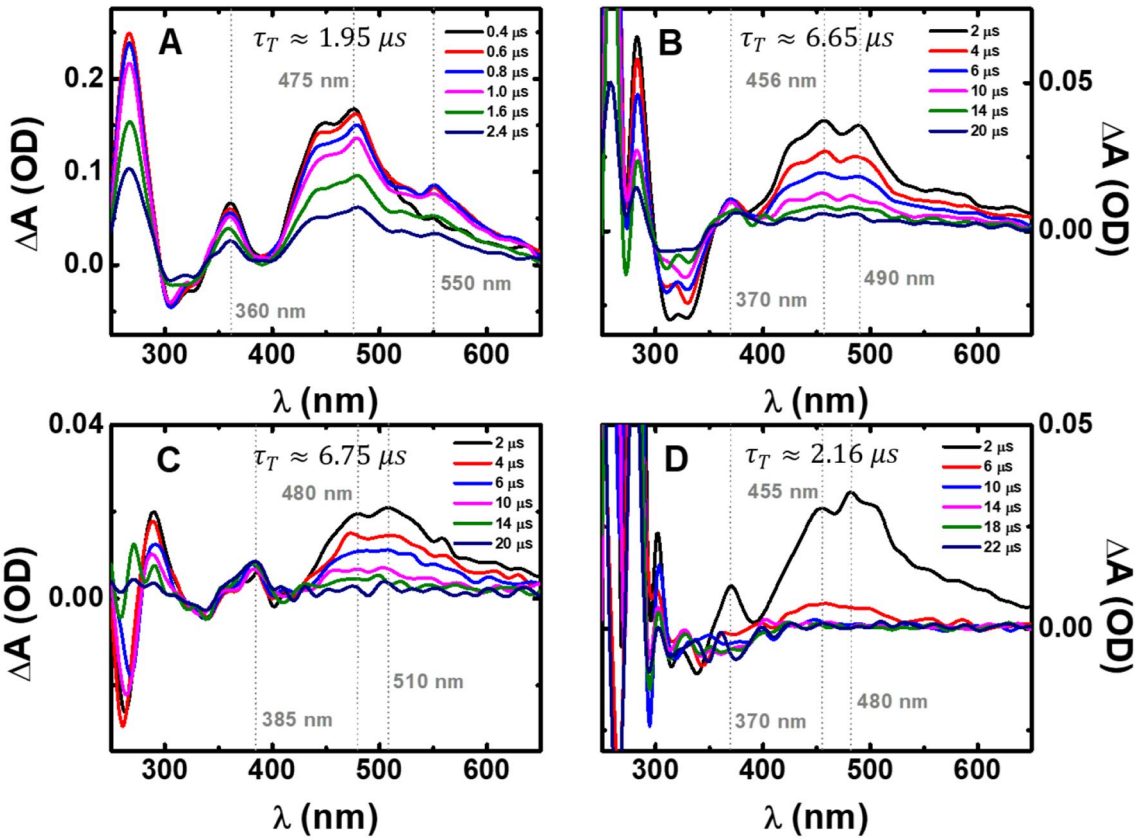

Fig. 3 Room-temperature transient singlet–triplet difference absorption spectra and triplet lifetimes obtained by nanosecond-microsecond transient absorption spectra (ns-TA) for TRYP (**A**), TRYP-2Br (**B**), TRYP-4Br (**C**) and TRYP-I (**D**) collected with excitation at 355 nm in degassed MeCN solutions at $T = 293$ K

Table 3 Room temperature time resolved fluorescence data (lifetimes, τ_i, normalized pre-exponential factors, a_{ij}, and Chi squared values, χ^2) obtained with picoseconds time-correlated single photon counting (ps-TCSPC) technique for the different tryptanthrin derivatives in solutions with oxygen, collected with excitation, λ_{exc}, ranging from 409 to 451 nm and at different emission wavelengths (along the emission band)

Compound	λ_{exc} (nm)	Solvent	λ_{em} (nm)	τ_1 (ps)	τ_2 (ps)	a_1	a_2	X^2
TRYP[a]	411	**MecN**	480	65	499	0.15	0.85	1.06
			510			0.11	0.89	1.16
			630			0.05	0.95	1.12
	422	**EtOH**	490	23	255	0.78	0.22	1.07
			540			0.42	0.59	0.92
			620			−0.27	1.00	0.91
	409	**MeOH**	500	12	146	0.73	0.27	1.23
			550			0.25	0.75	1.13
			600			−0.48	1.00	1.34
TRYP-2Br	422	**MeCN**	460	15	109	0.39	0.61	1.02
			510			0.28	0.72	0.96
		EtOH	480	12	193	0.89	0.10	1.21
			530			0.56	0.45	1.09
			570			0.33	0.67	1.09
		MeOH	480	12	174	0.86	0.14	1.00
			540			0.36	0.64	0.93
			570			0.19	0.81	1.03
TRYP-4Br	422	**MeCN**	480	7	119	0.80	0.20	1.13
			540			0.61	0.39	1.10
			580			0.52	0.48	0.99
		EtOH	500	12	89	0.91	0.09	1.14
			550			0.75	0.25	1.23
			590			0.58	0.42	1.10
		MeOH	500	10	68	0.88	0.12	1.05
			570			0.42	0.58	1.14
			610			−0.23	1.00	1.18
TRYP-I	422	**MeCN**	490	12	82	0.56	0.44	1.10
			550			0.53	0.46	1.29
			590			0.48	0.51	1.14
		EtOH	510	8	40	0.94	0.06	1.23
			570			0.68	0.32	0.94
		MeOH	560	13	41	0.66	0.34	0.96
			600			0.36	0.64	1.07
TRYP-NH_2	451	**MeCN**	520		2987		1.00	1.25
			590				1.00	1.10
			700				1.00	1.10
		EtOH	640		1144		1.00	1.23
			750				1.00	1.27
		MeOH	630		832		1.00	1.10
			740				1.00	1.12

[a]For TRYP data is from ref. [7]

Global analysis of the data revealed that, with the exception of TRYP-NH_2, the fluorescence decays are well fitted with sums of two exponentials, Eq. 3.

$$I(t) = a_1 e^{-t/\tau_1} + a_2 e^{-t/\tau_2} \quad (3)$$

The time-resolved data, summarized in Table 3, show, in the different studied solvents, the existence of a shorter fluorescence decay time (τ_2), found in the 7–65 ps range, together with a long-lived component (τ_1), in the 68–499 ps range, (Figure SI19-21 in SI). The data revealed that, while, with TRYP [7] a rising component (negative pre-exponential

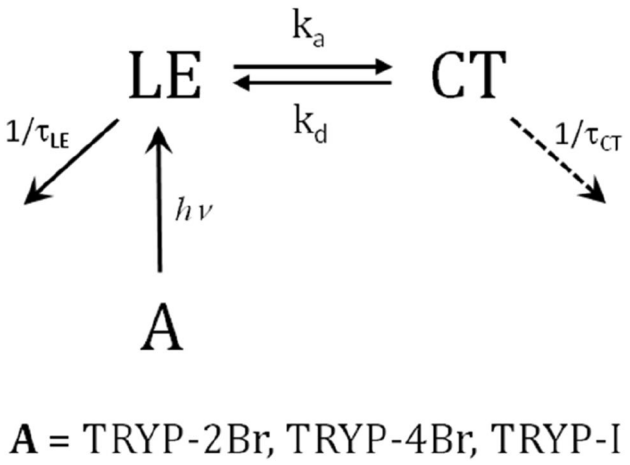

Scheme 3 Kinetic scheme for the excited behaviour of TRYP-2Br, TRYP-4Br and TRYP-I in S_1

value) is observed when the decays are collected at the longer wavelength emission in polar protic solvents, which was attributed to the formation, in the excited state, of a charge transfer (CT) at the expenses of a locally excited (LE) species (see Scheme 3), for the presently studied tryptanthrin derivatives, despite the double exponential nature of the decays, the presence of a rising component is only clearly observed for TRYP-4Br in MeOH (Table 3).

The data reveal that while, the decay time associated to the CT species (longer component, τ_1) decreases with number of Br atoms and from Br to I, reflecting the inductive effect of the halogen atoms, the shorter decay component, associated with the LE species (τ_2), is less dependent on the substitution and nature of the solvent. The absence of negative pre-exponential values in the fluorescence decays is attributed to a strong overlap of LE and CT band emission. This is also observed for TRYP in acetonitrile (Table 3) [7].

It is worth stressing that, as with TRYP [7], it is also possible to obtain, for tryptanthrin derivatives, the rate constants for the interconversion in the excited state of the two species: formation (k_a) of the CT at the expenses of the LE and deactivation (k_d and k_{CT}) of the CT and LE ($k_{LE} = 1/\tau_{LE}$) species (see Table 4).

In Table 4, the λ_i values are the reciprocal decay times of the shorter ($\lambda_2 = 1/\tau_2$) and of the longer ($\lambda_1 = 1/\tau_1$) species and are related to the rate constants in Scheme 3. The complete set of equations for the determination of the k_a, k_d, k_{LE} (which is assumed to have the value for a model compound, indigo, with a value of 152 ps [10]) and k_{CT} can be found in ref. [7] and these depends on the λ values and normalized pre-exponential factors at the shortest emission wavelength (which is related to the *A* value ($= a_{12}/a_{11}$) in Table 4.

Despite the fact that the k_a rate constant have values of ~ 10^{10}–10^{11} s^{-1} (values typically associated to charge transfer mechanisms) they are found to increase with the number (bromine) and atomic number (bromine to iodine), thus indicating a dominance of the ISC to the overall decay of the LE species (Table 4). The reversibility rate constant k_d remains approximately constant with the substitution whereas the k_{CT} values increase in the order TRYP-2Br > TRYP-4Br > TRYP-I, again in agreement with the more radiationless nature of the CT species [7].

In contrast with TRYP and the other tryptanthrin analogues, TRYP-NH_2 shows single-exponential decays in all solvents, with longer fluorescence lifetime values that vary from 0.8 ns to ~ 3.0 ns (Table 3). Moreover, the strong solvent polarity dependence (Fig. 1, Table 2) is likely to be associated to the emission of the CT state, indicating that upon photoexcitation, a very fast charge transfer occurs, faster than 1 ps (the time resolution of our ps-TCSPC setup), leading to the formation, and subsequent decay, of the relaxed CT state, but now in a ns time range, which contrasts with the other compounds (Table 3).

Table 4 Time-resolved data (λ_1, λ_2 and A) and rate constants (k_a, k_d and k_{CT}) recovered the kinetic analysis resulting from Scheme 3

Compound	Solvent	λ_1	λ_2	A	$k_a(ns^{-1})$	$k_d(ns^{-1})$	$k_{CT}(ns^{-1})$
TRYP[a]	EtOH	3.92	43.14	3.55	27.93	9.45	3.10
	MeOH	7.85	59.27	2.70	38.81	13.43	8.30
TRYP-2Br	EtOH	5.18	83.42	8.75	68.82	8.18	5.01
	MeOH	5.76	83.42	6.25	66.12	10.85	5.63
TRYP-4Br	EtOH	11.21	86.63	10.63	73.56	6.08	11.61
	MeOH	14.72	102.38	7.40	85.37	9.44	15.72
TRYP-I	EtOH	25.31	118.54	15.88	106.44	4.55	26.28
	MeOH	24.48	77.66	1.94	52.97	11.99	30.60

[a]For TRYP data is from ref [7]

4 Conclusions

A green chemistry procedure with microwave irradiation of indigo dyes allowed the synthesis of tryptanthrin derivatives with two and four bromine atoms, allowing the decrease of the E-factor to less than a half. Mono-substituted amine and iodine tryptanthrin derivatives were obtained, at room temperature, in a straightforward procedure from isatin and isatoic anhydride. The photophysical study showed that, with exception of TRYP-NH_2, the main excited state deactivation pathway is, for all the halogenated-tryptanthrin, intersystem crossing to the triplet state with highly efficient sensitization of singlet molecular oxygen, with yields, ϕ_Δ values higher than 80%.

Supplementary Information The online version contains supplementary material available at https://doi.org/10.1007/s43630-021-00117-8.

Acknowledgements This work was supported by Project "Hylight" (no. 031625) 02/SAICT/2017, PTDC/QUI-QFI/31625/2017, which is funded by the Portuguese Science Foundation (FCT) and Compete Centro 2020. The Coimbra Chemistry Centre (CQC) is supported by FCT, through Projects UIDB/00313/2020, and UIDP/00313/2020. We acknowledge the UC-NMR facility for obtaining the NMR data (www.nmrccc.uc.pt).

Declarations

Conflict of interest The authors declare that there is no conflict to interest.

References

1. Jahng, Y. (2013). Progress in the studies on tryptanthrin, an alkaloid of history. *Archives of Pharmacal Research, 36*(5), 517–535. https://doi.org/10.1007/s12272-013-0091-9
2. Tucker, A. M., & Grundt, P. (2012). The chemistry of tryptanthrin and its derivatives. *ARKIVOC, 1*, 546–569. https://doi.org/10.1002/chin.201243254
3. Jao, C.-W., Lin, W.-C., Wu, Y.-T., & Wu, P.-L. (2008). Isolation, structure elucidation, and synthesis of cytotoxic tryptanthrin analogues from *Phaius mishmensis*. *Journal of Natural Products, 71*(7), 1275–1279. https://doi.org/10.1021/np800064w
4. Hashimoto, T., Aga, H., Chaen, H., Fukuda, S., & Kurimoto, M. (1999). Isolation and Identification of Anti-*Helicobacter Pylori* Compounds from *Polygonum Tinctorium* Lour. *Journal of Natural Medicines, 53*(1), 27–31.
5. Rasmussen, L. E., Lee, T. D., Daves, J., & Schmidt, M. J. (1993). Female-to-male sex pheromones of low volatility in the Asian elephant Elephas Maximus. *Journal of Chemistry Ecology, 19*(10), 2115–2128. https://doi.org/10.1007/BF00979651
6. Honda, G., Tosirisuk, V., & Tabata, M. (1980). Isolation of an antidermatophytic, tryptanthrin, from indigo plants, polygonum tinctorium and isatis tinctoria. *Planta Medica, 38*(03), 275–276. https://doi.org/10.1055/s-2008-1074877
7. Pinheiro, D., Pineiro, M., Pina, J., Brandão, P., Galvão, A. M., & Seixas de Melo, J. S. (2020). Tryptanthrin from indigo: synthesis, excited state deactivation routes and efficient singlet oxygen sensitization. *Dyes Pigments, 175*, 108125. https://doi.org/10.1016/j.dyepig.2019.108125
8. Seixas de Melo, J. S. (2020). The molecules of colour and art. molecules with history and modern applications. In A. Albini & S. Prodi (Eds.), *Photochemistry* (Vol. 47, pp. 196–216). The Royal Society of Chemistry.
9. Seixas de Melo, J. S. (2018). The molecules of colour. In A. Albini, E. Fasani, & S. Protti (Eds.), *Photochemistry* (pp. 68–100). The Royal Society of Chemistry.
10. Pina, J., Sarmento, D., Accoto, M., Gentili, P. L., Vaccaro, L., Galvão, A. M., & Seixas de Melo, J. S. (2017). Excited-state proton transfer in Indigo. *Journal of Physical Chemistry B, 121*(10), 2308–2318. https://doi.org/10.1021/acs.jpcb.6b11020
11. Seixas de Melo, J. S., Rondão, R., Burrows, H. D., Melo, M. J., Navaratnam, S., Edge, R., & Voss, G. (2006). Spectral and photophysical studies of substituted indigo derivatives in their keto forms. *ChemPhysChem, 7*(11), 2303–2311. https://doi.org/10.1002/cphc.200600203
12. Onambele, L. A., Riepl, H., Fischer, R., Pradel, G., Prokop, A., & Aminake, M. N. (2015). Synthesis and evaluation of the antiplasmodial activity of tryptanthrin derivatives. *International Journal for Parasitology: Drugs and Drug Resistance, 5*(2), 48–57. https://doi.org/10.1016/j.ijpddr.2015.03.002
13. Hwang, J.-M., Oh, T., Kaneko, T., Upton, A. M., Franzblau, S. G., Ma, Z., Cho, S.-N., & Kim, P. (2013). Design, synthesis, and structure-activity relationship studies of tryptanthrins as antitubercular agents. *Journal of Natural Products, 76*(3), 354–367. https://doi.org/10.1021/np3007167
14. Kawakami, J., Kakinami, H., Matsushima, N., Nakane, A., Kitahara, H., Nagaki, M., & Ito, S. (2013). Structure-activity relationship analysis for antimicrobial activities of tryptanthrin derivatives using quantum chemical calculations. *Journal of Computer Chemistry Japan, 12*(2), 109–112. https://doi.org/10.2477/jccj.2012-0026
15. Kawakami, J., Matsushima, N., Ogawa, Y., Kakinami, H., Nakane, A., Kitahara, H., Nagaki, M., & Ito, S. (2011). Antibacterial and antifungal activities of tryptanthrin derivatives. *Transactions of the Materials Research Society of Japan*, *36*(4), 603–606. https://doi.org/10.14723/tmrsj.36.603
16. Bandekar, P. P., Roopnarine, K. A., Parekh, V. J., Mitchell, T. R., Novak, M. J., & Sinden, R. R. (2010). Antimicrobial activity of tryptanthrins in *Escherichia coli*. *Journal of Medicinal Chemistry, 53*(9), 3558–3565. https://doi.org/10.1021/jm901847f
17. Bhattacharjee, A. K., Hartell, M. G., Nichols, D. A., Hicks, R. P., Stanton, B., van Hamont, J. E., & Milhous, W. K. (2004). Structure-activity relationship study of antimalarial indolo [2,1-*b*] quinazoline-6,12-diones (tryptanthrins) three dimensional pharmacophore modeling and identification of new antimalarial candidates. *European Journal of Medicinal Chemistry, 39*(1), 59–67. https://doi.org/10.1016/j.ejmech.2003.10.004
18. Bhattacharjee, A. K., Skanchy, D. J., Jennings, B., Hudson, T. H., Brendle, J. J., & Werbovetz, K. A. (2002). Analysis of stereoelectronic properties, mechanism of action and pharmacophore of synthetic Indolo[2,1-b]quinazoline-6,12-dione derivatives in relation to antileishmanial activity using quantum chemical, cyclic voltammetry and 3-D-QSAR CATALYST procedures. *Bioorganic and Medicinal Chemistry, 10*(6), 1979–1989. https://doi.org/10.1016/S0968-0896(02)00013-5
19. Patil, S., Mane, A., & Dhongade-Desai, S. (2018). Ultrasound assisted synthesis of tryptanthrins catalyzed by zinc oxide nanoparticles. *Chemistry Science Review Letter, 7*(27), 732–740.
20. Catanzaro, E., Betari, N., Arencibia, J. M., Montanari, S., Sissi, C., De Simone, A., Vassura, I., Santini, A., Andrisano, V., Tumiatti, V., De Vivo, M., Krysko, D. V., Rocchi, M. B. L., Fimognari, C., & Milelli, A. (2020). Targeting topoisomerase II with tryptanthrin derivatives: discovery of 7-((2-(dimethylamino)ethyl)amino)

indolo[2,1-*b*]quinazoline-6,12-dione as an antiproliferative agent and to treat cancer. *European Journal of Medicinal Chemistry, 202*, 112504. https://doi.org/10.1016/j.ejmech.2020.112504
21. Hao, Y., Guo, J., Wang, Z., Liu, Y., Li, Y., Ma, D., & Wang, Q. (2020). Discovery of tryptanthrins as novel antiviral and anti-phytopathogenic-fungus agents. *Journal of Agriculture and Food Chemistry, 68*(20), 5586–5595. https://doi.org/10.1021/acs.jafc.0c02101
22. Li, Y., Zhang, S., Wang, R., Cui, M., Liu, W., Yang, Q., & Kuang, C. (2020). Synthesis of novel tryptanthrin derivatives as dual inhibitors of indoleamine 2,3-dioxygenase 1 and tryptophan 2,3-dioxygenase. *Bioorganic and Medicinal Chemistry Letters, 30*(11), 127159. https://doi.org/10.1016/j.bmcl.2020.127159
23. Wang, D., Xiao, F., Zhang, F., Huang, H., & Deng, G.-J. (2020). Copper-catalyzed aerobic oxidative ring expansion of isatins: a facile entry to isoquinolino-fused quinazolinones. *Chinese Journal of Chemistry*. https://doi.org/10.1002/cjoc.202000368
24. Deryabin, P. I., Moskovkina, T. V., Shevchenko, L. S., & Kalinovskii, A. I. (2017). Synthesis and antimicrobial activity of tryptanthrin adducts with ketones. *Russian Journal of Organic Chemistry, 53*(3), 418–422. https://doi.org/10.1134/s1070428017030174
25. Kaur, R., Manjal, S. K., Rawal, R. K., & Kumar, K. (2017). Recent synthetic and medicinal perspectives of tryptanthrin. *Bioorganic & Medicinal Chemistry, 25*(17), 4533–4552. https://doi.org/10.1016/j.bmc.2017.07.003
26. Krivogorsky, B., Nelson, A. C., Douglas, K. A., & Grundt, P. (2013). Tryptanthrin derivatives as toxoplasma *gondii* Inhibitors–structure–activity-relationship of the 6-position. *Bioorganic and Medicinal Chemistry Letters, 23*(4), 1032–1035. https://doi.org/10.1016/j.bmcl.2012.12.024
27. Sriraman, K., Novak, M. J., Baum, J. C., Herron, A., & Olson, J. A. (2013). Surface behavior and imaging of the lowest unoccupied molecular orbital of Indolo[2,1-*b*]quinazoline-6,12-dione (tryptanthrin) via scanning tunneling microscopy. *Surface Science, 616*, 110–114. https://doi.org/10.1016/j.susc.2013.06.010
28. Liang, J. L., Park, S.-E., Kwon, Y., & Jahng, Y. (2012). Synthesis of benzo-annulated tryptanthrins and their biological properties. *Bioorganic and Medicinal Chemistry, 20*(16), 4962–4967. https://doi.org/10.1016/j.bmc.2012.06.034
29. Novak, M. J., Clayton Baum, J., Buhrow, J. W., & Olson, J. A. (2006). Scanning tunneling microscopy of indolo[2,1-*b*]quinazolin-6,12-dione (tryptanthrin) on HOPG: evidence of adsorption-induced stereoisomerization. *Surface Science, 600*(20), L269–L273. https://doi.org/10.1016/j.susc.2006.07.036
30. Pinheiro, D., Pineiro, M., & Seixas de Melo, J. S. (2021). Sulfonated tryptanthrin anolyte increases performance in pH neutral aqueous redox flow batteries. *Communications Chemistry, 4*(1), 89. https://doi.org/10.1038/s42004-021-00523-0
31. Fang, Y.-P., Lin, Y.-K., Su, Y.-H., & Fang, J.-Y. (2011). Tryptanthrin-loaded nanoparticles for delivery into cultured human breast cancer cells, MCF7: the effects of solid lipid/liquid lipid ratios in the inner core. *Chemical and Pharmaceutical Bulletin, 59*(2), 266–271. https://doi.org/10.1248/cpb.59.266
32. Kawakami, J., Osanai, C., & Ito, S. (2020). Photophysical properties of 2-hydroxytryptanthrin analog as a near-infrared dye for fluorescent imaging. *Transactions of the Materials Research Society of Japan, 45*(1), 19–22. https://doi.org/10.14723/tmrsj.45.19
33. Kawakami, J., Sasagawa, M., & Ito, S. (2018). 2-Hydroxy-1-((2-(pyridin-2-yl)hydrazono)methyl)tryptanthrin as a Fluorescent Chemosensor for Metal Ions. *Transactions of the Materials Research Society of Japan*, *43*(3), 209–212.https://doi.org/10.14723/tmrsj.43.209
34. Kawakami, J., Kinami, Y., Takahashi, M., & Ito, S. (2018). 2-Hydroxytryptanthrin and 1-Formyl-2-hydroxytryptanthrin as fluorescent metal-ion sensors and near-infrared fluorescent labeling reagents. *Transactions of the Materials Research Society of Japan*, *43*(2), 109–112. https://doi.org/10.14723/tmrsj.43.109
35. Kawakami, J., Tsuiki, A., Ito, S., & Kitahara, H. (2016). Naphthalene ring-fused 2-aminotryptanthrin as a fluorescent chemosensor for Al^{3+}. *Transactions of the Materials Research Society of Japan, 41*(1), 131–133. https://doi.org/10.14723/tmrsj.41.131
36. Kawakami, J., Takahashi, M., Ito, S., & Kitahara, H. (2016). Photophysical properties of the 2-hydroxytryptanthrin and its sodium salt as near-infrared dyes for fluorescent imaging. *Analytical Sciences Japan*, *32*(2), 251–253. https://doi.org/10.2116/analsci.32.251
37. Kawakami, J., Soma, A., Kikuchi, K., Kikuchi, Y., Ito, S., & Kitahara, H. (2014). 2-Aminotryptanthrin derivative with pyrene as a FRET-based fluorescent chemosensor for metal ions. *Analytical Sciences Japan, 30*(10), 949–954. https://doi.org/10.2116/analsci.30.949
38. Kawakami, J., Kikuchi, K., Chiba, K., Matsushima, N., Yamaya, A., Ito, S., Nagaki, M., & Kitahara, H. (2009). 2-Aminotryptanthrin derivative with pyrene as a FRET-based fluorescent chemosensor for Al^{3+}. *Analytical Sciences Japan*, *25*(12), 1385–1386. https://doi.org/10.2116/analsci.25.1385
39. Brandão, P., Pinheiro, D., Seixas de Melo, J. S., & Pineiro, M. (2020). I2/NaH/DMF as Oxidant *trio* for the synthesis of tryptanthrin from indigo or isatin. *Dyes Pigments, 173*, 107935. https://doi.org/10.1016/j.dyepig.2019.107935
40. Dubois, J. T., & Wilkinson, F. (1963). Radiative lifetime of triplet biacetyl. *The Journal of Chemical Physics, 39*(4), 899–901. https://doi.org/10.1063/1.1734389
41. Montalti, M., Credi, A., Prodi, L., & Gandolfi, M. T. (2006). *Handbook of photochemistry 3rd* (Edition). Taylor & Francis Group.
42. Seixas de Melo, J. S., Pina, J., Dias, F. B., & Maçanita, A. L. (2013). Experimental techniques for excited state characterisation. In H. D. Burows (Ed.), *Applied Photochemistry* (pp. 533–585). Springer.
43. Martínez, C. G., Neuner, A., Martí, C., Nonell, S., Braun, A. M., & Oliveros, E. (2003). Effect of the media on the quantum yield of singlet oxygen ($O_2(^1\Delta g)$) production by *9H*-Fluoren-9-one: solvents and solvent mixtures. *Helvetica Chimica Acta, 86*(2), 384–397. https://doi.org/10.1002/hlca.200390039
44. Pina, J., Seixas de Melo, J. S., Burrows, H. D., Maçanita, A. L., Galbrecht, F., Bünnagel, T., & Scherf, U. (2009). Alternating binaphthyl−thiophene copolymers: synthesis, spectroscopy, and photophysics and their relevance to the question of energy migration versus conformational relaxation. *Macromolecules, 42*(5), 1710–1719. https://doi.org/10.1021/ma802395c
45. Striker, G., Subramaniam, V., Seidel, C. A. M., & Volkmer, A. (1999). Photochromicity and fluorescence lifetimes of green fluorescent protein. *The Journal of Physical Chemistry B, 103*(40), 8612–8617. https://doi.org/10.1021/jp991425e
46. Seixas de Melo, J. S., & Barroso, M. (2001). Síntese, espectroscopia e tingimento com corantes: O Índigo. *Boletim da Sociedade Portuguesa da Química, 81*, 66–69.
47. Gaboriaud-Kolar, N., Nam, S., & Skaltsounis, A.-L. (2014). Progress in the chemistry of organic natural products. In H. Falk, A. Kinghorn, & J. Kobayashi (Eds.), *A colourful history: the evolution of indigoids.* Springer.
48. Sheldon, R. A. (2017). The E factor 25 years on: the rise of green chemistry and sustainability. *Green Chemistry, 19*(1), 18–43. https://doi.org/10.1039/C6GC02157C
49. Kawakami, J., Kawaguchi, H., Kikuchi, K., Yamaya, A., Ito, S., & Kitahara, H. (2013). Fluorescent solvatochromism of 2-aminotryptanthrin. *Transactions of the Materials Research Society of Japan*, *38*(1), 123–125. https://doi.org/10.14723/tmrsj.38.123
50. Kawakami, J., Osanai, C., & Ito, S. (2018). Fluorescence emission mechanism of three N, N-dimethylaminotryptanthrins by density

functional theory calculations. *Transactions of the Materials Research Society of Japan*, *43*(5), 319–323. https://doi.org/10.14723/tmrsj.43.319

51. Kawakami, J., Kadowaki, T., Ikeda, M., Habata, Y., Ito, S., & Kitahara, H. (2016). Spectral characteristics of highly fluorescent 2-(*N, N*-dimethylamino)tryptanthrin. *Transactions of the Materials Research Society of Japan*, *41*(2), 143–146. https://doi.org/10.14723/tmrsj.41.143
52. Seixas de Melo, J. S., & Fernandes, P. F. (2001). Spectroscopy and photophysics of 4- and 7-hydroxycoumarins and their thione analogs. *Journal of Molecular Structure, 565–566*, 69–78. https://doi.org/10.1016/S0022-2860(01)00458-6
53. El-Sayed, M. A. (1968). Triplet state-its radiative and nonradiative properties. *Accounts of Chemical Research, 1*(1), 8–16. https://doi.org/10.1021/ar50001a002
54. Dang, H., Hou, X., Roos, P., & Nielsen, S. P. (2013). Release of iodine from organic matter in natural water by $K_2S_2O_8$ oxidation for ^{129}I determination. *Analytical Methods, 5*(2), 449–456. https://doi.org/10.1039/C2AY25958C
55. Hacobian, S., & Iredale, T. (1950). Role of oxygen in the photolysis of iodides. *Nature, 166*(4212), 156–157. https://doi.org/10.1038/166156b0